

Löwdin Transform on FCC Optimized UWB Pulses

Philipp Walk

Heinrich-Hertz-Lehrstuhl für Informations-,
theorie und theoretische Informationstechnik, TU,
Einsteinufer 25, 10587 Berlin
Email: philipp.walk@mk.tu-berlin.de

Peter Jung

Fraunhofer German-Sino Lab for
Mobil Communications, MCI,
Einsteinufer 37, 10587 Berlin
Email: peter.jung@hhi.de

Jens Timmermann

Institut für Hochfrequenztechnik und
Elektronik Universität Karlsruhe, TH,
Kaiserstrasse 12, 76131 Karlsruhe
Email: jens.timmermann@ihe.uka.de

Abstract—In this contribution we present a novel method for constructing orthogonal pulses for UWB impulse radio transmission under the FCC spectral mask constraint. In contrast to previous work we combine a convex formulation of the spectral design with Löwdin’s orthogonalization method [1], which delivers a shift-orthogonal basis optimally close (in energy) to the initial pulse, which generates (in a stable way) the shift-invariant space. The convex formulation of the spectral design is achieved by approximating the FCC mask with a finite-order filter matched to Gaussian monocycles as input. The output pulse then has high energy concentration in the passband (NESP value). Using Löwdin’s orthogonalization we compute the corresponding shift-orthogonal pulse. We show that our approach is able to generate for finitely many shifts, orthogonal equal energy pulses with nearly the same NESP value. Furthermore, we show that the orthogonalization procedure can be well approximated using the Zak transform allowing for an efficient implementation with the discrete Fourier transform. Surprisingly, we could observe, that for certain parameters, this approximation yields almost the same performance as the exact Löwdin method.

Index Terms—Löwdin transformation, UWB impulse radio, Zak transform, shift-invariant spaces, PPM

I. INTRODUCTION

Ultra-wideband (UWB) radio transmission has gained increasing interest in recent years for short-range indoor wireless communication. UWB aims for high data rates at short distances at a very low power density. A promising technology is the impulse radio UWB system that uses nanosecond pulses to transmit information. Typical pulses in this setting are for example the Gaussian monocycle. But, the power spectral density (PSD) of the pulses must be controlled to be compatible with the spectral mask released by the Federal Communication Commission (FCC) or the ITU. To achieve a power efficient operation of UWB devices it is therefore necessary to further shape the pulse such that the FCC mask is utilized as much as possible. On the other hand orthogonality of pulses is desirable for channelization, for example when multiple systems [2] or users will use the same spectrum. Moreover, the performance in bit error rate (BER) for fixed energy per bit of M -ary orthogonal signal design in a memoryless AWGN channel increases with M assuming that all signals possess the same energy and support in time [3, Ch.4]. A shift-invariant structure in the orthogonal and spectral efficient signaling is advisable in order to have simple and low-cost filter implementations.

In this context, the UWB pulse design problem can then also be stated as follows: Suppose that we already have a certain set of linear independent pulses, for example a set of

equidistant translates of a basic pulse, as is used for pulse position modulation (PPM) in UWB systems. For an infinite number of translates such a set will be called shift-invariant in what follows. There exist several ways to obtain an orthogonal basis having the same span. A famous example is the Gram-Schmidt procedure [2], which depends on a particular ordering of the pulse translates. However, in this procedure different pulse translates are distorted differently and the orthogonal pulses usually do not retain a shift-invariant structure, i.e. cannot be used directly for PPM.

On the other hand there exist democratic (i.e. order independent) methods, where all given signals are handled simultaneously. The canonical and symmetric orthogonalization of Löwdin [4] are such methods. In the finite-dimensional setting, these approaches are optimal in an averaged L^2 -sense, i.e. minimizing the overall sum of energy distortions [5]. For a certain class, these ideas can also be extended to the infinite-dimensional case, i.e. orthogonal bases which are L^2 -close to Riesz bases (known as Bari bases). However, for infinite-dimensional shift-invariant systems this approach cannot work as for example already stated in [6]. In this paper we therefore present a method to compute a particular pulse, which generates a shift-orthogonal set and has minimal error (in energy) with respect to the initial pulse.

The paper is organized as follows: After introducing the system model we present in Section II the optimization of the basic UWB pulse to the FCC mask. In Section III we consider the orthogonalization of this optimized pulse with respect to its translates. Finally, Section IV presents the implementation results of our optimization and orthogonalization method to a Gaussian monocycle, which is an UWB relevant setting.

Signal Model

In UWB impulse radio transmission one uses pulse amplitude modulation or PPM [7], [8]. Both modulation strategies yield a PSD of the radiated UWB signal u , which is a amplified version of the square of the power spectrum of the basic pulse p . In this work, we will only consider the M -ary PPM method [9]. If we omit the time hopping code the PPM-transmitted waveform is:

$$u(t) = \sum_n \sqrt{\frac{\mathcal{E}}{\mathcal{E}_p}} p(t - nT_s - d_n T), \quad (1)$$

where \mathcal{E} denotes the desired transmitted energy per pulse and \mathcal{E}_p the energy of the basic pulse p . The time shift T is the pulse position modulation factor. The M -ary sequence $\{d_n\}$ is a wide-sense stationary random process, where each random variable d_n is assumed to be equally likely distributed and corresponds to the n th information data symbol. Each d_n takes integer values between 0 and $M - 1$ with equal probability, i.e. $\log_2 M$ bits of information. T_s is the symbol duration, in our case the pulse repetition time, which is much greater than the length T_p of the support of p . To avoid intersymbol interference we must, in fact, meet the requirement $T_s \geq (M - 1)T + T_p$. One way to decrease the symbol error rate, is to increase the energy per symbol, i.e. the energy \mathcal{E} of the radiated signals. But this leads to a violation of the FCC mask. Another way to improve the overall performance is to increase M , since this increases the data rate by $\log_2 M$, as long as pulse orthogonality can be ensured. But decreasing the modulation shift T below T_p results in an overlap of the translates. If the overlapping translates can be designed to be orthogonal to each other, the performance can be increased further (see for example [3, (4.95)]).

II. PULSE SHAPE OPTIMIZATION TO THE FCC MASK

We are interested in a maximization of the average power of UWB signals in a certain passband F_p . The average power is a quadratic functional in the pulse spectrum \hat{p} (\hat{p} denotes here the Fourier transform of p). The target functional is the PSD of the UWB signal integrated over the passband F_p :

$$\tilde{\eta}(p) := \int_{F_p} |\hat{p}(f)|^2 df. \quad (2)$$

Since the PSD is limited by the FCC to the mask $S_{\text{FCC}}(f)$ in a certain frequency range $F := [0 \dots 14]\text{GHz}$, we have to impose the constraints (in the following we set $\mathcal{E} = \mathcal{E}_p T_s$ [7]):

$$|\hat{p}(f)|^2 \leq S_{\text{FCC}}(f) \quad \text{for all } f \in F. \quad (3)$$

The FCC frequency mask for indoor UWB is shown in Fig. 1. The optimization of $\eta := \tilde{\eta} / \int_{F_p} |S_{\text{FCC}}(f)|^2 df$ is also known as the direct maximization of the normalized effective signal power (NESP) value [10].

Pulse shapes with large NESP values η can be constructed by using an appropriate filter. As the first step of our proposed pulse shape optimization we will compute such a filter with a method similar to the one already presented in [7]. Assume that q is a time-limited, continuous and realizable pulse. Filtering with a L 'th order real filter $\mathbf{g} \in \mathbb{R}^L$ with coefficients g_k results in the pulse:

$$p(t) = \sum_{k=0}^{L-1} g_k q(t - kT_0) \quad \text{for } t \in \mathbb{R}. \quad (4)$$

For fixed pulse q , time-shift T_0 and filter order L the optimization problem for the NESP value is given by:

$$\begin{aligned} \max_{\mathbf{g} \in \mathbb{R}^L} \tilde{\eta} \left(\sum_{k=0}^{L-1} g_k q(\cdot - kT_0) \right) \\ \text{s.t. } \forall f \in F : |\hat{p}(f)|^2 = |\hat{g}(f)|^2 \cdot |\hat{q}(f)|^2 \leq S_{\text{FCC}}(f), \end{aligned} \quad (5)$$

where \hat{q} is the Fourier transform of the filter g . The solution \mathbf{g} then defines with (4) the optimal pulse under FCC constraints. Reformulating (5) in terms of the symmetric filters auto-correlation $\mathbf{r} \in \mathbb{R}^L$ results in a linear problem with linear matrix inequality constraints [11]. This is achieved by the fact, that the power spectrum of the filter is the Fourier transform of the auto-correlation:

$$|\hat{g}(f)|^2 = \Phi_{gg}(f) = \sum_{n=0}^{L-1} r_n \phi_n(f),$$

with $\phi_0(f) := 1$ and $\phi_n(f) := 2 \cos(2\pi T_0 n f)$ for $n \geq 1$. Equation (5) reads now as the following semi-infinite linear problem:

$$\max_{\mathbf{r} \in \mathbb{R}^L} \sum_n r_n c_n, \quad \text{s.t. } \forall f \in F: 0 \leq \Phi_{gg}(f) \leq M(f). \quad (6)$$

with $M(f) := S_{\text{FCC}}(f) / |\hat{q}(f)|^2$ and constants $c_n := \int_{F_p} |\hat{q}(f)|^2 \phi_n(f) df$. For each f the inequalities in (6) describe a half plane in \mathbb{R}^L . Let us now split these double inequalities into six inequality constraints. The lower bound, being the necessary condition for \mathbf{r} to define a valid auto-correlation function, is given by:

$$\Phi_{gg}(f) \geq 0 \quad \text{for } f \in F. \quad (7)$$

Next, we partition the interval F into five piecewise constant FCC mask sections¹ $F_i = [\alpha_i, \beta_i]$ as in [12] yielding the following upper bounds:

$$\Phi_{gg}(f) \leq M(f) \quad \text{for } f \in F_i \quad (8)$$

Since $M(f)$ is in general not a finite polynomial, we approximate $M(f)$ on each section F_i in the basis of the L scaled trigonometric polynomials ϕ_n in the L^2 -norm by $\Gamma_i(f) := \sum_n \gamma_n^i \phi_n(f)$. Obviously, this is only an approximation to the original problem (see here also [12, eq. (23)]). The vector γ^i of coefficients $\{\gamma_n^i\}_{n=0}^{L-1}$ is determined for each $i = 1 \dots 5$ by:

$$\min_{\gamma^i \in \mathbb{R}^L} \left\{ \int_{\alpha_i}^{\beta_i} \left| M(f) - \sum_{n=0}^{L-1} \gamma_n^i \phi_n(f) \right|^2 df \right\}. \quad (9)$$

The constraints $\Phi_{gg}(f) \leq \Gamma_i(f)$ are now semi-infinite linear and describe a compact convex set, which can be formulated as cones [11, (40) + (41)] for $\theta \in F$:

$$K_l(\theta) = \left\{ \mathbf{r} \left| \sum_{n=0}^{L-1} r_n \phi_n(f) \geq 0, f \in \left[\theta, \frac{1}{2T_0} \right] \right. \right\}.$$

For $\theta = 0$ the positive cone $K_0 = K_l(0)$ defines the lower bound in (7) if we set $T_0 = \frac{1}{28 \text{GHz}}$. To formulate the non-constant upper bounds one can use the approximation functions Γ_i [12] which are given in the same basis $\{\phi_n\}$ as the power spectrum Φ_{gg} . The bounds in (8) are then equivalent to the following linear inequalities:

$$\sum_{n=0}^{L-1} (\gamma_n^i - r_n) \phi_n(f) \geq 0, \quad f \in [\alpha_i, \beta_i].$$

¹ $\Gamma_1 \dots \Gamma_4$ could overlap since the FCC mask divided by the Gaussian monocycle power spectrum is monotone increasing on $[0, 10.6]$ GHz.

So for the upper bounds, we just have to set

$$p_n^i := \gamma_n^i - r_n \text{ for } n \geq 1, \quad (10)$$

which leads to the upper bound cones

$$K_u(\theta_i) = \left\{ \mathbf{r} \mid \sum_{n=0}^{L-1} p_n^i \phi_n(f) \geq 0, f \in \left[\theta_i, \frac{1}{2T_0} \right] \right\}$$

$$\bar{K}_u(\theta_i) = \left\{ \mathbf{r} \mid \sum_{n=0}^{L-1} p_n^i \phi_n(f) \geq 0, f \in [0, \theta_i] \right\}.$$

The five upper bounds are then

$$K_1 = \bar{K}_u(1.61), \quad K_2 = \bar{K}_u(1.99), \quad K_3 = \bar{K}_u(3.1), \quad (11)$$

$$K_4 = \bar{K}_u(10.6), \quad K_5 = K_u(10.6).$$

Since the auto-correlation \mathbf{r} must fulfill all these constraints, it must be an element of the intersection of all convex sets $K := \bigcap_{i=0}^5 K_i$, hence the constraint for \mathbf{r} is a positive bounded cone. The problem in (5) can then be approximated² as:

$$\max_{\mathbf{r} \in K} \tilde{\eta}(\mathbf{r}). \quad (12)$$

This is now a convex optimization problem in \mathbf{r} of a linear functional $\tilde{\eta}(\mathbf{r}) = \sum r_n c_n$ over the convex intersection set K . These cone constraints can be formulated with an extended version of the positive real lemma [11] as a semi-definite program (SDP). This problem is then numerically solvable with the MATLAB toolbox SeDuMi [13], [14]. In Fig. 1 the functions Γ_i are shown for a Gaussian monocycle q multiplied by a triangle function Λ to yield a smooth time-limited pulse q_Λ , see section IV.

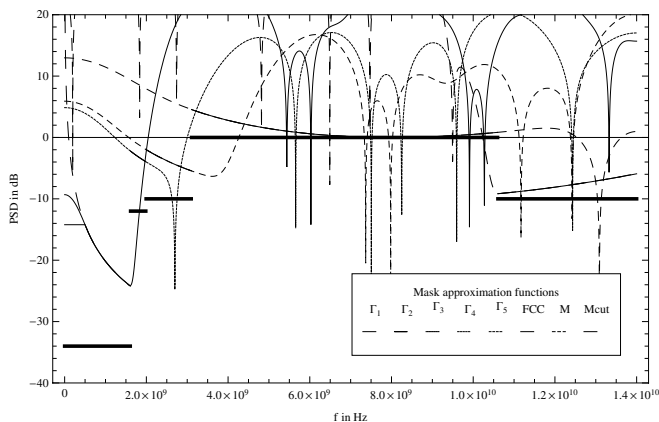


Figure 1. Piecewise Fourier approximation $\Gamma_i(f)$ of order $L = 31$ of the adjusted FCC mask $M(f)$ with a triangle-masked Gaussian monocycle q_Λ .

² Since $\{\Gamma_i\}_{i=1}^5$ are approximations for the upper bounds, they still result in a certain mask violation which needs to be compensated (see Section IV). Also, T_0 is now fixed to the frequency range F . So reducing T_0 needs a reformulation of the cones, hence $\{\gamma_i\}_{i=1}^5$ and an extension of the frequency band constraints. Furthermore, increasing T_0 above 1/28 GHz is not desirable for full mask control.

III. PULSE ORTHOGONALIZATION

In the following we present now the second step of our pulse shape design. Let us consider a finite set $\{p(\cdot - kT)\}_{k=-M}^M$ of $2M + 1$ equally spaced translates (shifts) of the optimal pulse p given by (4) and (12). Since equally spaced translates are linear independent, see [15], this set is a basis for its $2M + 1$ dimensional span $V_{MT}(p)$. We propose now an orthogonalization method, known as Löwdin orthogonalization [1], to transform this set of translates by a linear operation to an orthonormal basis (ONB) $\{p_k^{\circ, MT}\}_{k=-M}^M$ for $V_{MT}(p)$ s.t. the average energy distortion $\sum_{k=-M}^M \|p(\cdot - kT) - p_k^{\circ, MT}\|_2^2$ with respect to p is minimized (with $\|\cdot\|_2^2$ we denote the squared L^2 -norm, i.e. the energy). The Löwdin transform is given by:

$$p_n^{\circ, MT} := \sum_{m=-M}^M [\mathbf{G}_{MT}^{-\frac{1}{2}}]_{nm} p(\cdot - nT) \quad (13)$$

Here, $\mathbf{G}_{MT}^{-\frac{1}{2}}$ denotes the inverse square root of the $2M + 1 \times 2M + 1$ dimensional Gram-Matrix \mathbf{G}_{MT} with components:

$$[\mathbf{G}_{MT}]_{nm} := \int_{-\infty}^{\infty} p(t - mT) \overline{p(t - nT)} dt. \quad (14)$$

Note that $\{p_k^{\circ, MT}\}_{k=-M}^M$ is usually not a set of translates of a certain single function. Furthermore, the distortion of these pulse shapes with respect to the original shape will depend on the decay properties of the (initial) optimal pulse and the amount of overlap. In the next sections, we will fix the time shift by $T = 1$ s.t. the overlap is controlled by the decay properties.

Shift-Invariant Spaces

To investigate the stability for $M \rightarrow \infty$ of the Löwdin transform in (13) we need the formalism of shift-invariant spaces $V(p)$ (being the L^2 -closure of $V_\infty(p)$). They are defined as closed linear subspaces of L^2 invariant under integer translation. We will call p a generator of $V(p)$.

Our goal is now to find a new pulse $p^\circ \in V(p)$ s.t. the set of its infinitely many translates $\{p^\circ(\cdot - n)\}$ is an ONB for $V(p)$ where we then call p° an orthonormal generator of $V(p)$. Furthermore, the set $\{p(\cdot - n)\}$ is called a Riesz basis if the Gram matrix $\mathbf{G} := \mathbf{G}_\infty$ is a bounded positive invertible operator from $\ell^2(\mathbb{Z})$ (the Hilbert space of square-summable sequences) into itself and in this case $V(p)$ is a closed subspace of L^2 . In this setting it is well known [16] that a continuous pulse p generates a Riesz basis if there exist constants $0 < A \leq B < \infty$, such that:

$$A \leq \sum_{j \in \mathbb{Z}} |\hat{p}(\nu + k)|^2 = \mathbf{Z}(p * \bar{p}_-)(0, \nu) \leq B \quad (15)$$

holds for almost every frequency $\nu \in \mathbb{R}$. The function $p_-(t) := p(-t)$ denotes here the time reversal of p . If $A = B$, the pulse p is already an orthogonal generator [17, Th. 7.2.3] and (15) is then known as the Nyquist condition. As already indicated in (15) these conditions can also be

expressed in terms of the Zak transform [18] which is in case of a continuous function f defined as:

$$(\mathbf{Z}f)(t, \nu) := \sum_{k \in \mathbb{Z}} f(t - k) e^{2\pi i k \nu}. \quad (16)$$

Note that (15) contains the Zak transform of the auto-correlation of p . Its samples are given by the Gram Matrix:

$$r_p(n - m) := (p * \bar{p}_-)(n - m) = [\mathbf{G}]_{nm}. \quad (17)$$

In particular, r_p is the auto-convolution of p if the pulse is Hermitian (this means $\bar{p}(-t) = p(t)$). If we further assume that p and \hat{p} are both in the Wiener space $W(\mathbb{R})$, i.e. $L^\infty(\mathbb{R})$ -functions with norm:

$$\|p\|_W := \sum_{k \in \mathbb{Z}} \text{ess sup}_{t \in [0,1]} |p(t - k)| < \infty, \quad (18)$$

then they are continuous and (15) holds pointwise [16, p.105]. To further emphasize this fact, we denote by $W_0(\mathbb{R})$ the space of continuous Wiener functions, where the locally boundedness implies a globally one. In the next section we can show, that for certain compact supported Wiener pulses, which are generating a Riesz basis for $V(p)$, our finite construction in (13) converges pointwise and yield an orthonormal generator p° for $V(p)$.

Stability and Approximation

The limit $\{p_n\}$ of the initial pulse set $\{p_n\}_{n=-K}^K$ for $K \rightarrow \infty$ is shift-invariant, hence the Riesz and Nyquist conditions are expressed in terms of \hat{p} . This suggests a straightforward construction of an orthogonalization procedure with the discrete Fourier transform (DFT). However, for any finite K , shift-invariance can only be achieved by cyclic extension, and then it is not clear whenever such an approach is also stable.

Theorem (Stability of Löwdin Orthogonalization). *Let $M \in \mathbb{N}$ and $p, \hat{p} \in W_0(\mathbb{R})$, such that*

- (i) $\text{supp}(p) \subset [-\frac{M}{2}, \frac{M}{2}]$ and
- (ii) $\{p(\cdot - k)\}_{k \in \mathbb{Z}}$ is a Riesz basis for $V(p)$

holds. Then the limit of the Löwdin orthogonalization $\{p_k^\circ\}$, can be approximated by the sequence $\{\hat{p}_k^{\circ,K}\}_{k=-K}^K$, which is represented pointwise for $K \geq M$ and each $k \in [-K, K]$ by:

$$\hat{p}_k^{\circ,K}(t) := \begin{cases} \sum_{l=0}^{2K} \frac{e^{-\frac{2\pi i k l}{2K+1}} (\mathbf{Z}p)(t, \frac{l}{2K+1})}{\sqrt{(\mathbf{Z}r_p)(0, \frac{l}{2K+1})}}, & |t| \leq K + \frac{M}{2}, \\ 0, & \text{else} \end{cases}, \quad (19)$$

such that for each $k \in \mathbb{Z}$:

$$p^\circ(t - k) = \lim_{K \rightarrow \infty} \hat{p}_k^{\circ,K}(t) \quad (20)$$

converges for each $t \in \mathbb{R}$ (i.e. pointwise) and defines a shift-orthonormal-set.

A detailed proof of this theorem is given in [19]. We sketch in this contribution only the following ideas of the proof:

Due to the compact support of p and the condition $K \geq M$, the Gram matrix \mathbf{G}_K is a banded Toeplitz matrix, and because p is also bounded the limit $K \rightarrow \infty$ in (13) can be

understood pointwise. Using the techniques ("finite section method") by Strohmer and Christensen [20] it can be shown that the sequence of inverse square roots of the Strang circulant preconditioners [21] $\{\tilde{\mathbf{G}}_K\}$ is an applicable approximation method for the inverse square root of \mathbf{G} whenever $\{p(\cdot - k)\}$ is a Riesz basis for $V(p)$.

Since p and \hat{p} are Wiener functions, the condition on the spectral function $\Phi(\nu) := \sum_k |\hat{p}(\nu + k)|^2$ in (15) holds pointwise. From the compactness argument and (15) the eigenvalues $\tilde{\lambda}_l^K$ of the circulant matrix [21] $\tilde{\mathbf{G}}_K$ are given as integer samples of Φ :

$$\begin{aligned} \tilde{\lambda}_l^K &:= \sum_{n=-M}^M r_p(n) e^{-2\pi i n \frac{l}{2K+1}} \\ &\stackrel{(16)}{=} (\mathbf{Z}r_p)(0, \frac{l}{2K+1}) \stackrel{(15)}{=} \Phi(\frac{l}{2K+1}) \end{aligned} \quad (21)$$

Thus, in the limit this is the "orthogonalization trick" [22] in the frequency domain:

$$\hat{p}^\circ(\nu) = \frac{\hat{p}(\nu)}{\sqrt{\sum_m |\hat{p}(\nu + m)|^2}}.$$

Hence, the pulse fulfils the Nyquist condition.

Discussion of the Riesz Condition

The key property in the theorem is the Riesz basis condition (15) which together with the Wiener condition establishes the strict positivity $\Phi(\nu) \geq A > 0$ of the trigonometric polynomial:

$$\Phi(\nu) = r_p(0) + 2 \sum_{k=1}^M r_p(k) \cos(2\pi k \nu) \quad (22)$$

on $\nu \in [0, 1]$ since the optimal pulse p is real-valued (r_p is defined in (17)). Analytical methods for the construction of positive trigonometric polynomials is a long-standing problem [23] and can be guaranteed only for certain exactly given sequences $\{r_p(k)\}$ (e.g. for exponential sequences) or with further convexity assumptions. Rough estimates of the form $r_p(0) - 2 \sum_{k=1}^M |r_p(k)| \leq \Phi(\nu)$ usually fail due to the alternating behavior of the sequence and the cosine. Finally we note that it seems to be more promising to impose another SDP formulation on the $r_p(k)$. This will result in a more complicated problem structure due to the intertwining of the two transformation (4) and (19).

IV. ALGORITHMIC IMPLEMENTATION

In (4) we used the Gaussian monocycle which is given by [2, p.107]:

$$q(t') = \frac{-2A_q t'}{\sigma^3 \sqrt{\pi}} e^{-(\frac{t'}{\sigma})^2} \quad \text{for } |t'| \leq \frac{T_q}{2} \quad (23)$$

where the width σ and the amplitude A_q is chosen s.t. $|\hat{q}(f)|^2$ attains its maximum 1 at 6.85GHz (the center of F_p) and the support length T_q is chosen s.t. it contains 99.99% of the total energy:

$$\sigma = 6.85 \text{ GHz}/\sqrt{2\pi} \quad \text{and} \quad T_q = 4.95\sigma \text{ sec.} \quad (24)$$

Note that simple truncation yields non-continuous pulses and a bad decay in the frequency domain. To ensure the Wiener conditions for p in (4) we now mask q by a unit triangle pulse Λ of width T_q , i.e. we set $q_\Lambda(t') := \Lambda(t') \cdot q(t')$. This results in the same support, but in a faster frequency decay, s.t. $q_\Lambda, \hat{q}_\Lambda \in W_0(\mathbb{R})$. This remains true for any finite linear combination, hence for p .

In the following we consider only odd filter orders L for the procedure in (12). Then we can center p in its support $[-\frac{T_p}{2}, \frac{T_p}{2}]$ where $T_p := (L-1)T_0 + T_q$. If we set $t' := t T_p/M$ we obtain the scaled FIR filtered pulse:

$$p(t) = \sum_{k=-\frac{L-1}{2}}^{\frac{L-1}{2}} g_k q_\Lambda \left(t \frac{T_p}{M} - k T_0 \right) \quad \text{for} \quad |t| \leq \frac{M}{2} \quad (25)$$

Thus, $T = 1$ corresponds to a time shift of T_p/M seconds for the unscaled pulse, which results in $2M+1$ overlapping shifts contained in $[-3T_p/2, 3T_p/2]$.

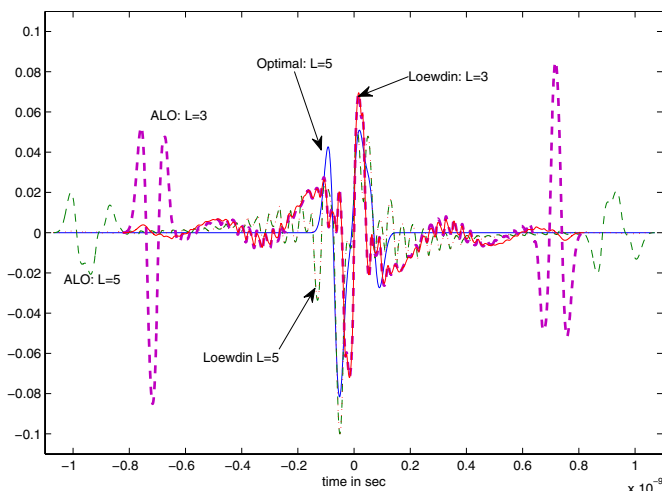


Figure 2. Optimal (from (12)), LO and ALO pulse shapes for filter order $L = 3$ and $L = 5$. We used here $K = 3M$ and $M = 8$.

For each $K \geq M$ the pulses in (19) are K -approximations to the Löwdin orthogonal (LO) pulses $p^\circ(\cdot - k)$. We will call these approximations in the following approximated Löwdin orthogonal (ALO) pulses of order K . How well $\{\tilde{p}_0^{\circ,K}(\cdot - k)\}$ is approximating a shift-orthogonal set? For this we computed with MATLAB the ALO pulses by using the DFT.

In Fig. 2 we show for filter order $L = 3$ and $L = 5$ the ALO pulses $\tilde{p}^{\circ,K}$ together with the initial pulse p and the LO pulses $p^{\circ,K}$ of order $K = 3M$ with $M = 8$. It can be observed that $\tilde{p}^{\circ,K}$ and $p^{\circ,K}$ are quite similar but have increased support as compared to p . But, due to the circulant construction, $p^{\circ,K}$ has slight more concentration at the boundaries which vanishes

with increasing K or L . In fact, for $K = 3M, L = 31$ there are no boundary effects for the ALO pulses visible, see Fig. 3.

In Fig. 4 the scaled PSD (power spectrum) of the ALO pulses are shown together with the FCC mask and the optimal pulse, which corresponds to a time-shift of $T := T_p/M = T_p$, i.e. $M = 1$. For $M = 8$ we plot also the LO pulse, which matches very well the corresponding ALO pulse.

In Fig. 5 we plot the NESP values for the ALO and LO pulse sets. Our mask approximation in Sec. II and the orthogonalization in Sec. III are both optimal in an L^2 -sense, but not automatically in the L^∞ -sense. Therefore we have to correct manually for the maximal amplitude factor s.t. each pulse is in compliance with the FCC mask. This results in a slightly reduced η . Nevertheless, it could also increase performance, like for $M = 2$ due to an equalizing property. An increasing of M , hence an increasing of the overlap, reduces the NESP values, except for $M = 8$, see Fig. 5. The reason for this behaviour comes from the intertwining of the two time shifts T_0 and T due to the two transformations, see the discussion of the theorem. For $M = 8$ we can transmit 17 orthogonal symbols with more than 82% spectral efficiency in the UWB passband. These are five times more symbols compared to traditional PPM.

In Fig. 6 we show the cross-correlation functions χ_{0l}^{24} for $l = 1, 2, 7$, which are given as:

$$\chi_{kl}^K(\tau) := \int \tilde{p}_k^{\circ,K}(t) \tilde{p}_l^{\circ,K}(t - \tau) dt.$$

The shift-orthogonal character of the ALO pulses is very sharp visible in Fig. 6, so $\tilde{p}_0^{\circ,K}$ is a promising candidate for an PPM pulse.

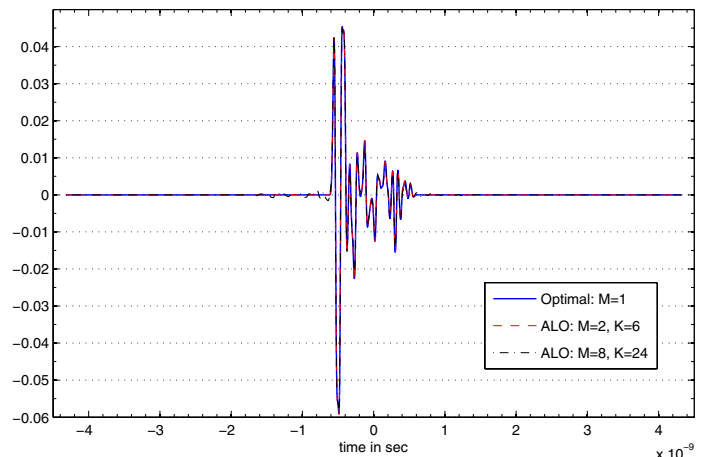


Figure 3. Optimized ALO pulse shapes of order $L = 31$ for various M .

V. CONCLUSIONS

We have presented a novel orthogonalization method for UWB impulse radio transmission. Contrary to prior work our method has the advantage of being order-independent, problem-size-independent and optimal in an L^2 -sense. We have shown that the shift-orthogonal basis can be well and stable approximated. Surprisingly, the ALO pulses

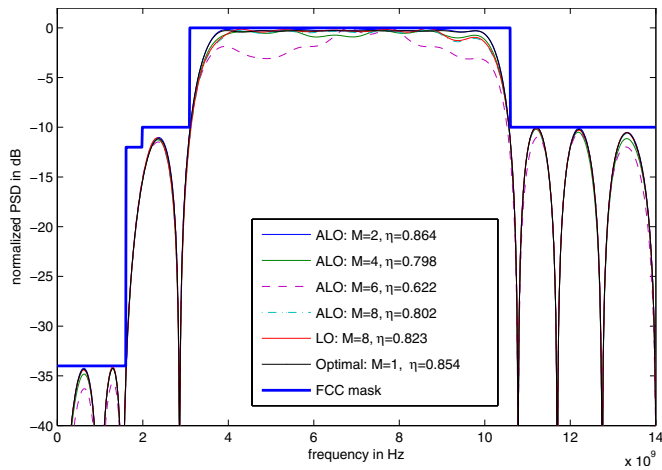


Figure 4. PSD of the 0th ALO and LO pulses for various M with $L = 31$.

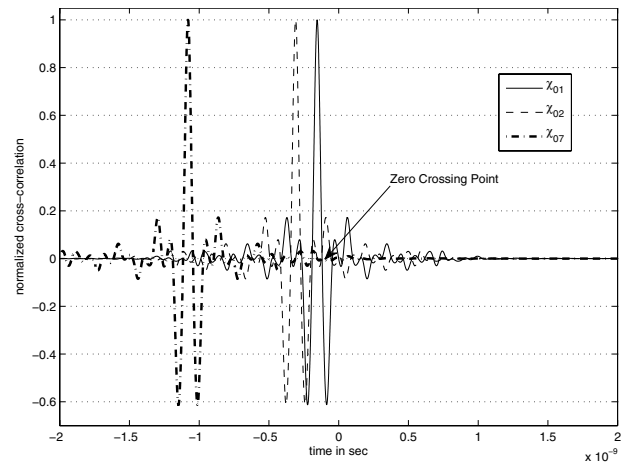


Figure 6. Cross-correlations of ALO pulses for $L = 31, M = 8$.

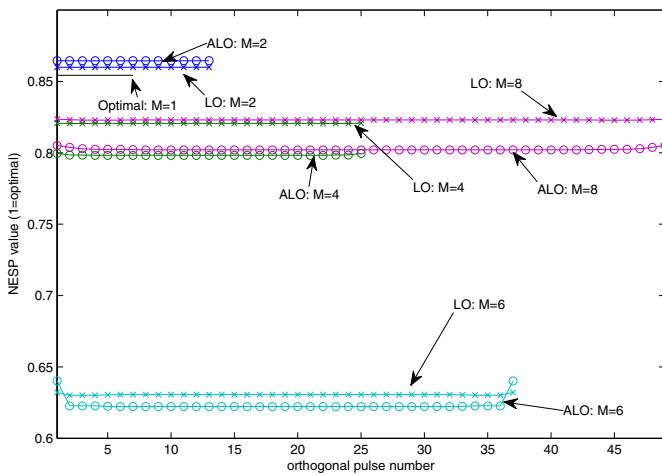


Figure 5. NESP values of ALO and LO pulse sets for $L = 31$ and $K = 3M$.

are at sufficiently high K and L almost identical to the LO pulses and seem even to obtain a better shift-invariant structure. Thus, our method provide a simple procedure of orthogonalizing overlapping UWB pulses.

ACKNOWLEDGEMENT

The authors wishes to thank Holger Boche and Brendan Farrell for their support.

REFERENCES

- [1] P.-O. Löwdin, "On the non-orthogonality problem connected with the use of atomic wave functions in the theory of molecules and crystals," *J. Chem. Phys.*, vol. 18, pp. 367–370, 1950.
- [2] Z. Tian, T. N. Davidson, X. Luo, X. Wu, and G. B. Giannakis, *Ultra Wideband Wireless Communication: Ultra Wideband Pulse Shaper Design*. Wiley, 2006.
- [3] M. K. Simon, S. M. Hinedi, and W. C. Lindsey, *Digital Communication Techniques: Signal Design and Detection*. Prentice Hall, 1994.
- [4] P.-O. Löwdin, "On the nonorthogonality problem," *Advances in Quantum Chemistry*, vol. 5, pp. 185–199, 1970.
- [5] G. Aiken, J. A. Erdos, and J. A. Goldstein, "On Löwdin orthogonalization," *Int. J. of Quantum Chemistry*, vol. 18, pp. 1101 – 1108, 1980.

- [6] A. Janssen and T. Strohmer, "Characterization and computation of canonical tight windows for gabor frames," *J. Fourier. Anal. Appl.*, vol. 8(1), pp. 1–28, 2002.
- [7] X. Luo, L. Yang, and G. B. Giannakis, "Designing optimal pulse-shapers for ultra-wideband radios," *Journal of Communications and Networks*, vol. 5, no. 4, pp. 344–353, December 2003.
- [8] M. Z. Win and R. A. Scholtz, "Impulse radio: how it works," *IEEE Commun. Lett.*, vol. 2, no. 2, pp. 36–38, February 1998.
- [9] B. L. Cho, M. M.-O. Lee, and T.-Y. Kim, "A new design and analysis of M-ary PPM UWB," *Lecture notes in computer science*, vol. 3079, pp. 685–695, 2004.
- [10] X. Wu, Z. Tian, T. Davidson, and G. Giannakis, "Optimal waveform design for UWB radios," *IEEE Trans. Signal Process.*, vol. 54, pp. 2009–2021, 2006.
- [11] T. Davidson, Z.-Q. Luo, and J. F. Sturm, "Linear matrix inequality formulation of spectral mask constraints with applications to FIR filter design," *IEEE Trans. Signal Process.*, vol. 50, no. 11, pp. 2702– 2715, 2002.
- [12] C. R. Berger, M. Eisenacher, H. Jakel, and F. Jondral, "Pulseshaping in UWB systems using semidefinite programming with non-constant upper bounds," in *IEEE Int. Symp. on Personal, Indoor and Mobile Radio Communications*, 2006.
- [13] S.-P. Wu, S. Boyd, and L. Vandenberghe, *Applied and Computational Control, Signals and Circuits: 5. FIR Filter Design via Spectral Factorization and Convex Optimization*, B. Datta, Ed. Birkhauser, 1999.
- [14] J. F. Sturm, "Using SeDuMi 1.02, a MATLAB toolbox for optimization over symmetric cones," *Optimization Methods and Software*, vol. 11, no. 1, pp. 625–653, 1999.
- [15] P. A. Linnell, "Von neumann algebras and linear independence of translates," *Journal of Proc. Amer. Math. Soc.*, vol. 127, pp. 3269–3277, 1999.
- [16] K. Gröchenig, *Foundations of Time-Frequency Analysis*. Springer Verlag, 2001.
- [17] O. Christensen, *An Introduction to Frames and Riesz Bases*. Birkhauser, 2003.
- [18] A. J. E. M. Janssen, "The Zak transform: A signal transform for sampled time-continuous signals," *Philips J. Res.*, vol. 43, pp. 23–69, 1988.
- [19] P. Walk and P. Jung, "Löwdin orthogonalization for UWB impulse radio," 2010, journal in preparation.
- [20] O. Christensen and T. Strohmer, "The finite section method and problems in frame theory," *Journal of Approximation Theory*, vol. 133, no. 2, pp. 221–237, April 2005.
- [21] R. Chan and G. Strang, "The asymptotic toeplitz-circulant eigenvalue problem," MIT App. Math. Dept., Numer. Anal. 87-5, 1987.
- [22] I. Daubechies, *Ten Lectures on Wavelets*. Regional Conference Series in Applied Mathematics, 1992.
- [23] D. K. Dimitrov, *Approximation Theory: A volume dedicated to Blagovest Sendov*. Sofia: Marin Drinov Academic Publishing House, 2004.